

Universal cosmic rays energy spectrum and the mass composition at the 'ankle' and above

T. Wibig

Faculty of Physics and Applied Informatics, University of Lodz, 90-256 Łódź, Poland.

A.W. Wolfendale

Department of Physics, Durham University, Durham, DH1 3LE, UK

(Dated: September 18, 2018)

We have used recently published data from the Pierre Auger Observatory and the Telescope Array Project to conclude some inferences concerning the origin and composition of ultra high-energy cosmic rays (UHECR). We advocate for model the UHECR flux as a combination of the Galactic and Extragalactic components exchanging the dominant role at the famous feature of the energy spectrum called 'the ankle'. We put a special emphasis on the individual experiment energy resolution and possible biases it introduces. We have eventually combined the data from both big experiments to the one 'world average' UHECR spectrum and we used it, supported by the analysis of the distribution of the Extensive Air Shower (EAS) development maximum depth to find the UHECR mass composition of both: Galactic and Extragalactic components. We studied the dependence of the on mass composition on the cosmic ray source distribution in space. We present results for some models existing in the literature. We found the evidence of the deficit of Extragalactic sources in the vicinity of the Galaxy of the the UHECR, what is in concordance with the small scale anisotropy analysis results.

I. INTRODUCTION

The question about the nature of the particles of energies around the spectral feature called the ‘ankle’ is one of the most important and still open questions in the Ultra High-Energy Cosmic Ray (UHECR) domain. The lower energy cosmic rays are known to be mainly confined within the Galaxy, and it is known that the Galactic field is too weak to contain particles of energies above 10^{19} eV. It is believed by us and others that the ‘ankle’ is related to the Extragalactic (EG) origin of the cosmic ray particles of ultra high energies.

The two biggest experiments Pierre Auger Observatory (PAO) and Telescope Array Project (TA) acting on the UHECR domain at present have been publishing the new data successively, for some time. The statistics of collected events increased substantially the accuracy of delivered results. Actually both groups gathered numbers of events which allow them to obtain the CR spectra with the accuracy limited mainly not by the aperture, but rather by the methodology of the data analysis including the accuracy of the Monte Carlo simulations (see, e.g., [1]). Further increase of statistics would improve, in principle, the determination of some particular shower characteristics as, e.g., the average depth of the shower maximum (X_{\max}) or its dispersion ($\text{rms}_{X_{\max}}$), but the general problems with theoretical description is still based and hung on simulations. The analysis of all existing data suggests that the problem now is not in the statistical uncertainty, but rather of the systematics in both: the measurements and the EAS modeling.

The recently published data from PAO [2–5] and TA [6–10] form the solid basis to search for conclusions concerning the origin and composition of UHECR (see, e.g., [11]). We would like to present here our analysis of data on cosmic ray spectra (shown in Fig.1) taken together together. We combined them to the one ‘world average’ UHECR spectrum and used as a one much more accurate datum which supported by the analysis of the $\langle X_{\max} \rangle$ and $\text{rms}_{X_{\max}}$ data measured also by both experiments which we show in Fig.2. The recent analysis of the widths of the X_{\max} distribution for narrow energy bins use the whole distributions as they are measured. The TA group does not report $\text{rms}_{X_{\max}}$ data. Published distributions are not corrected for the instrumental effects and their widths are considerably wider than values reported by other groups (e.g. HiRes [12] or PAO [11]), so we will use below only PAO data on $\text{rms}_{X_{\max}}$.

It is known for many years that spectra published by both big experiments do not agree with each other. Some unknown experimental bias (at least in the estimated shower energy) still exists and it is widely discussed, e.g., in Ref. [13]. Based on the recent analysis of both teams the bias is of order of ~ 0.1 in the $\log(E)$ scale what gives about $\sim 20\%$ (14% [3]) of the energy over(under)estimation error. There is of course no indication which spectrum should be used as a datum. Therefore our analysis will be presented two fold: once assuming that the PAO data is the one, once the TA measurement. We do not wish to judge which solution is closer to the reality, but we are going, first, to test what the uncertainty it makes concerning the mass composition of the ‘ankle’.

The conclusions of the recent PAO paper [13] and also by Taylor, Ahlers and Hooper [14, 15], Globus, Allard and Parizot [16] and others are obtained using only the PAO measurements. The TA Collaboration conclusions were formed, contrary, using only TA results [9, 17]. We would like to perform the examination of both: the spectra and composition data measured by the Pierre Auger Observatory and the Telescope Array experiment in the whole ‘ankle’ region where, in our opinion, the Galactic and Extragalactic components meet.

Our results and comparison with the other work conclusions will be commented in Sec.V.

II. THE UHECR FLUX MODEL

As the way proposed and successfully applied in Ref. [18]. The cosmic ray flux is assumed to be the sum of Galactic and Extragalactic components which cross at about the middle of the structure called ‘the ankle’, located roughly between the particle energies of 10^{18} and 10^{19} eV. Below the ankle, we assumed, that the cosmic rays originate mostly in our Galaxy. Galactic magnetic fields are strong enough and enough turbulent to confine cosmic ray particles of energies below 10^{18} eV and propagate them in the diffusive regime within the volume of the Galactic halo. Depending on the electric charge the confinement ends around 10^{18} eV and particles of higher energies leak out to intergalactic space. The Galactic (G) component energy spectrum is assumed to be a power-law with the index of about (-3) observed below 10^{17} eV modified by the rigidity dependent Galactic leakage factor which we have found to be roughly of the Gaussian shape [18]. The real structure of the Galactic component cut-off is probably much more complicated. At least it should be a sum of different nuclei fluxes, each with the cut-off at different total energy due to the most probable rigidity dependent mechanism of the leakage. The contribution of the source acceleration energy limit(s) is also possible here. Due to the lack of knowledge of all these processes we assumed just pure Gaussian cut-off shape with two parameters left to be adjusted in the fitting procedure. The form of the Galactic component is given by Eq. (1).

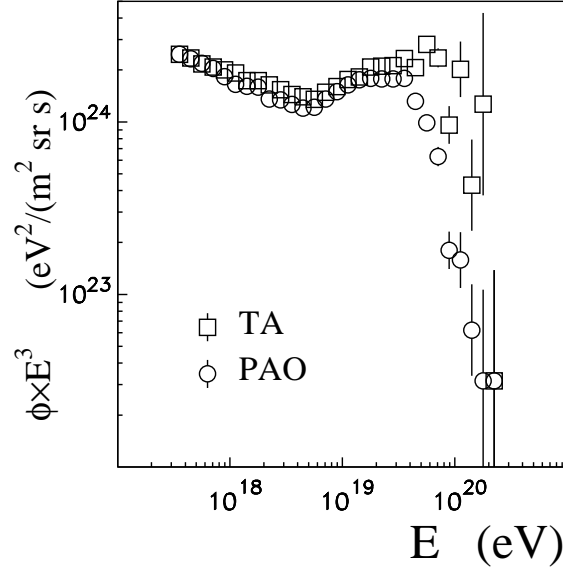


FIG. 1. Pierre Auger Observatory and Telescope Array Project UHECR energy spectra as they are reported recently by both groups.

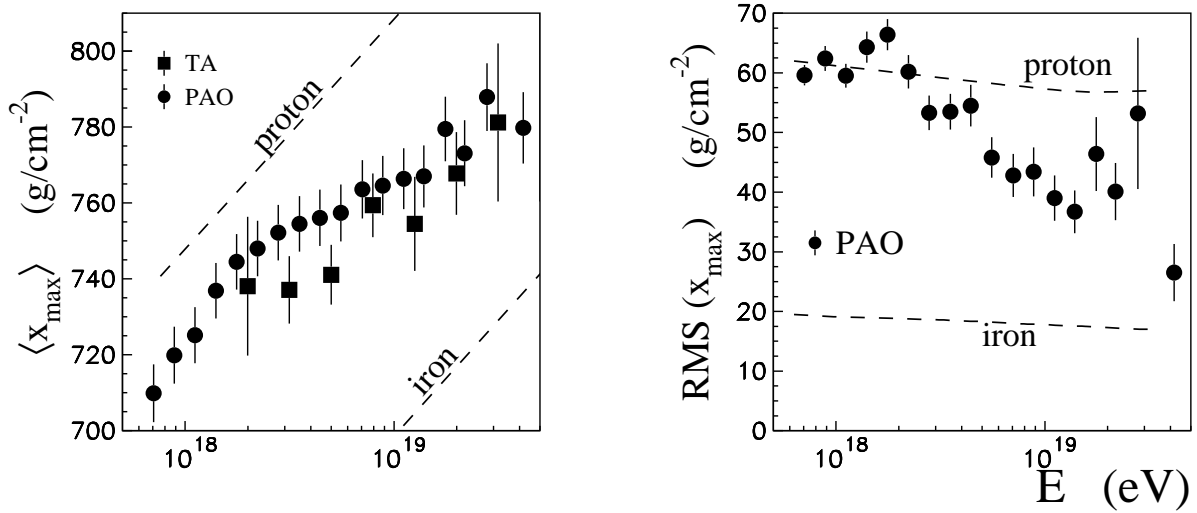


FIG. 2. PAO and TA data of the distribution of depth of the UHECR shower maxima: the average position of X_{max} and its spread: $\text{rms}_{X_{\text{max}}}$. Lines shows results of simulations for pure proton and iron showers made by the PAO Collaboration.

$$\Phi_G(E) = \Phi_{0G} E^{-\gamma_G} \times \begin{cases} 1 & \text{if } E < E_{G\text{cut}} \\ \exp\left(-\frac{(E - E_{G\text{cut}})^2}{2\sigma_G^2}\right) & \text{if } E > E_{G\text{cut}} \end{cases} \quad (1)$$

The Extragalactic (EG) component is consistently assumed to be also of the power-law form but harder, with the index of about (-2). Such a simply spectrum is supposed to work in the ankle region (and below), but for higher energies the cut off also exists, what is clearly visible in both discussed experiment spectra and shown in Fig.1. For

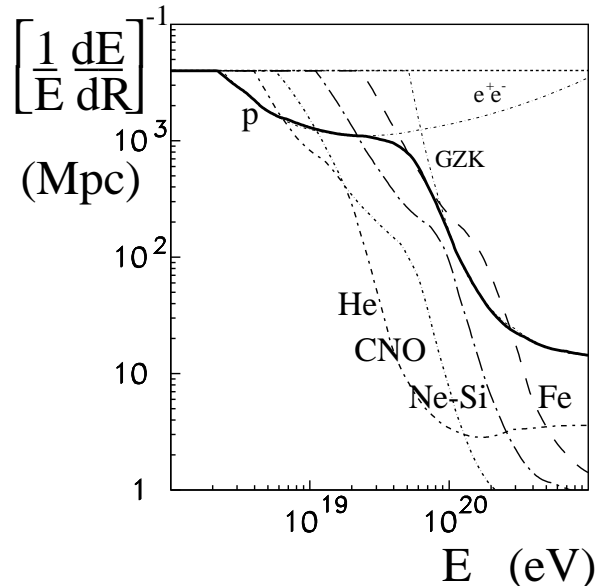


FIG. 3. The energy losses lengths for GZK and different nuclei photodisintegration processes.

the UHECR EG particles, if there are protons, nuclei or even some exotic particles like photons (which case we do not discussed in the present work), there exist well known physical mechanisms limiting their energies when they reach the Earth. In the case of protons the famous GZK cut-off [19, 20] works above few times 10^{19} eV. It is the consequence of the existence of the Δ resonance just in the energy region of collisions of the UHECR nucleons with photons of cosmic microwave background (CMB). Below the GZK cut-off energy there is expected the effect of e^+e^- pair production by the UHECR protons in the CMB. This effect is not as big and definite as GZK, but it should be taken into account for more detailed, e.g., mass composition, analysis.

For nuclei the giant dipole resonance existence leads to fast disintegration of UHECR nuclei passing through intergalactic photons of CMB but also interacting with the intergalactic photon field in infrared (IR) range. Unfortunately the IR light intensity (and the IR photon energy spectrum) is not known as well as the CMB radiation. The detail shape of the nuclei cut-off is a source of the theoretical uncertainty [21, 22] at the energies below the ones when the CMB smashes all nuclei fast and definitively. The physical processes listed above allows us to determine more exactly the shape of "the end of the cosmic ray spectrum":

The formula describing the EG UHECR flux adopted in the present analysis is shown in Eq.(2).

$$\Phi_{\text{EG}}(E) \frac{d\Phi_{\text{EG}}}{dE} = \Phi_{0\text{EG}} E^{-\gamma_{\text{EG}}} \times \begin{cases} f_{\text{GZK}} & \text{for protons} \\ f_{\text{nuc}} & \text{for nuclei} \end{cases} \quad (2)$$

where $f_{\text{GZK}}(E)$ and $f_{\text{nuc}}(E)$ are factors obtained numerically for the process of the energy losses of nucleons and nuclei which we shown in Fig.3. The energy loss lengths are calculated separately for protons and nuclei of the main four groups named as He, CNO, Ne-Si, and Fe, which contributions will be examined later on.

To get numerical values of the f factors in Eq.(2) the CR flux reaching us from the sources have to be integrated over their distribution in the space, which do not have to be uniform. We will come back to this point in Sec. IV A.

III. 'WORLD AVERAGE' UHECR SPECTRUM

All problems mentioned above make the situation at the "end of the spectrum" complicated, but we will try to answer all questions successfully. We will start from combining both spectra (PAO and TA) together, removing the mentioned above experimental biases.

Our analysis is based on the supposition that 'the ankle' is the real feature of the observed UHECR flux, and the flux is given by $\Phi_{\text{UHECR}} = \Phi_{\text{G}} + \Phi_{\text{EG}}$.

From the experimental point of view UHECR flux has been examined by many group, historically, from the important John Linsley measurement in Volcano Ranch [23], but actually mostly by PAO and TA, each having its own energy resolution and possible biases in estimated energy and collecting aperture. Both big contemporary working experiments are very complicated and the procedure of single shower energy determination is known in general, but there are plenty of instrumental and analysis details which are not widely known. Some of them are described in more or less technical papers [13, 24]. The 'concluding' experimental spectra are 'checked' finally with respective Monte Carlo. This, however, adds the MC code, and simulation approximation uncertainties to the overall uncertainty of the final results. There is no way to overcome all this, and we have to live with it.

The flux normalization discrepancy (vertical displacement) is also observed in the data (Fig.1), but it does not disturb our further composition analysis and conclusions. The energy bias is also simply factor, which the energy should be multiplied by. It does not change the shape of the spectrum, too. But the experimental energy resolution changes the theoretical expectations for each experiment differently. According to the experiment group reports the energy resolution is similar for PO and TA and it is of order 0.1 in the \log_{10} energy scale [3, 6]. In particular, of course, it depends on the actual sample of showers analyzed, the quality of events, and of the energy itself.

According to the simulations, e.g. [25], we assumed the energy reconstruction uncertainty to be Gaussian on the logarithmic scale. Transferring the UHECR universal flux reaching the Earth to the spectrum measured by the j -th experiment we have

$$\Phi_{\text{obs}_j}(E) = \int d(\log E') E' \Phi_{\text{UHECR}}(E') \frac{1}{\sqrt{2\pi}\sigma_j} \exp\left[-\frac{(\log(E) - \log(E'))^2}{2\sigma_j^2}\right] . \quad (3)$$

For the exact power-law UHECR spectrum $\Phi_{\text{UHECR}}(E) = E^{-\gamma}$ the effect of the folding it with the Gaussian resolution (on the $\log(E)$) does not change the shape, it remains power-law. It shifts only the spectrum up by the factor of $\exp(\gamma^2\sigma_j^2/2)$ on the flux intensity scale. However, if the spectrum has a more complicated structure it is eventually changed. The effect is obvious and was discussed already in [26] and by us in [18]. It makes the structures, generally smoothed. In the case of 'the ankle' it makes it less significant. When we combined spectra of many different experiments, each with its own, different resolution, this effect is very important and have to be taken into account if we wish to resolve the correct 'world average' UHECR spectrum. For the present analysis, we are going to combine only two spectra obtained by two EAS arrays with similar resolutions, the situation is simpler, but the effect still exists, what should be remembered.

The concept of the procedure is based, as it has been said, on the assumption, that the structure of 'the ankle' – the dip between the 10^{18} eV and 10^{19} eV, is the real phenomenon. Below the energy of 10^{19} eV the cut-off factors of the EG component shown in Eq.(2) do not contribute. If we, at the first step of combining PAO and TA spectra, limit the fitting procedure to the energies below 2×10^{19} using not all points measured by PAO and TA, the following four parameters of the Galactic component in Eq.(1) can be determined:

- normalization Φ_{0G}
- index γ_G
- position of the confinement cut-off $E_{G\text{cut}}$
- width of the confinement cut-off σ_G

and two Extragalactic component parameters describing the EG power-law in Eq.(2):

- normalization Φ_{0EG}
- index γ_{EG}

The parameters listed above, however, are not all parameters acting in the 'ankle' region. Two energy resolutions for both experiments together with one independent energy bias makes (if we took PAO energy measurement as a datum we set energy bias for PAO points to 0, and accordingly with the TA energy normalization) all together 9 parameters to be adjusted to the spectra of the 'ankle' measured by PAO (Φ_{PAO_i}) and TA (Φ_{TA_i}). The spectra in the energy range of interest ($\log(E)$ less than 19.2) consist of 16 points from PAO and TA data sets, each with its individual statistical uncertainty (Δ_i). The cost function which we try to minimize is the χ^2 defined conventionally as

$$\chi^2 = \sum_{\text{PAO}} ((\Phi_{\text{obsPAO}}(E_i) - \Phi_{\text{PAO}_i})/\Delta_{\text{PAO}_i})^2 + \sum_{\text{TA}} ((\Phi_{\text{obsTA}}(E_i) - \Phi_{\text{TA}_i})/\Delta_{\text{TA}_i})^2. \quad (4)$$

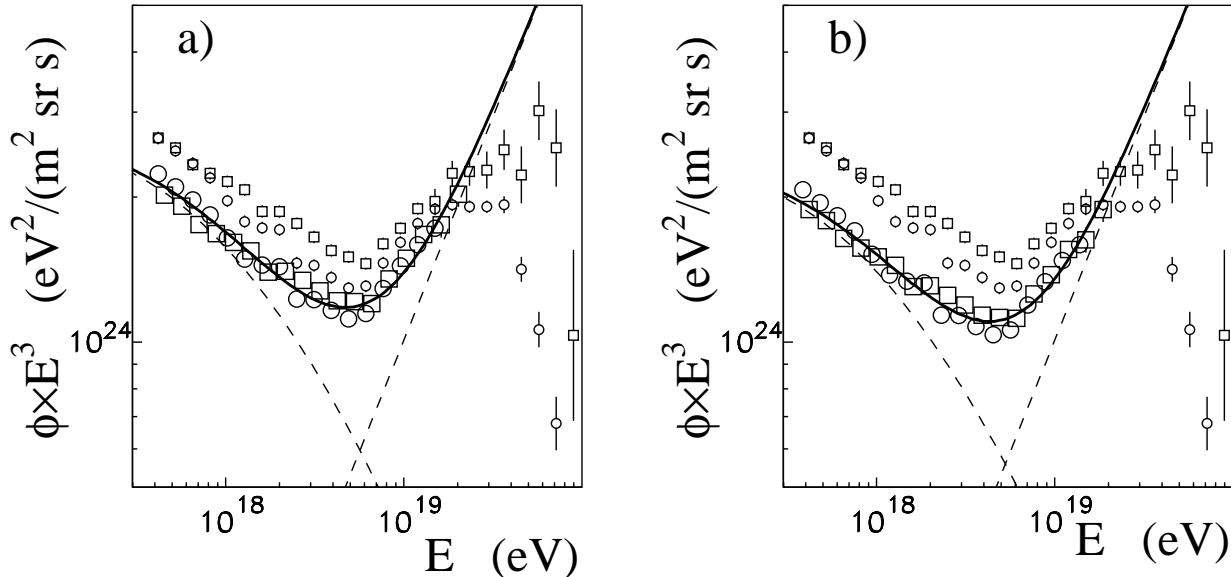


FIG. 4. Energy spectrum fits of the G and pure power-law EG components in the 'ankle' energy region. On the left plot - a), the absolute normalization reported by PAO is used and the systematic shifts are applied only for TA data. For the right plot - b), the opposite: the TA normalization is fixed and PAO is systematically shifted. The small symbols (circles for PAO and squares for TA) are the original measured spectra. The big symbols are the 'unfolded' spectra using the logarithmic slope of the model spectrum shown by solid black line.

Of course not all parameters are independent and the procedure of χ^2 minimization had to be made carefully consecutively in different parameter subspaces omitting local minima and divergences. Eventually we obtained two fits to the 'ankle' spectra for the PAO and the TA energy normalizations. They are showed in Fig.4. Each plot shows the universal UHECR spectrum adjusted to both sets of data but for different experiment energy estimation used as a datum. The original measured data points are shown by small symbols (circles for PAO, squares for TA) and the solid line represents the unfolded spectrum. The big symbols are the measured points 'corrected' by the experimental resolution of Eq.(3). The bias on the energy scale is set 0 for PAO points at the left plot, Fig.4a, and 0 for TA on the right one, Fig.4b. Dashed lines shows Galactic and Extragalactic components.

With the values of the model parameters found for the uncut EG component, we have calculated the universal UHECR spectrum $\Phi_{\text{UHECR}} = \Phi_{\text{G}} + \Phi_{\text{EG}}$ in the whole energy range. We used here, as an example for 'the end of the spectrum' cut-off the one calculated for the Fe group in the uniform CR source distribution. For other choices the results do not change significantly. This, more realistic spectrum shape is needed to shift each measured point accordingly. We did the calculations for both (PAO and TA) energy normalizations to get the local value of the logarithmic slope of the spectrum (γ) needed to unfold the measured spectra. It does not depend much on the particular choice of the cut-off shape (within reasonable limits) and the Fig.4 presents the situation for pure iron nuclei flux and uniform distribution of CR sources. More detail will be shown and discussed below in Sec. IV. The results of the unfolding procedure is shown in Fig.5. The 'universal UHECR spectra' are shown by the solid lines for both normalization cases: Fig.5a for PAO and Fig.5b for TA, respectively. Points (circles for PAO and squares for TA) represent 'unfolded data points' of both experiments.

As we can see in Figs.4 and 5 the 'unfolded' points from both measurements lie closely to the proposed universal UHECR spectrum, at least in the 'ankle' region. There is seen the small difference between the PAO and TA energy normalizations (left and right plots in Figs.4 and 5), but here the difference is only a systematic shift and we can combine the point from both experiments together. It has been done and the resulting universal 'world average' UHECR spectrum is shown in Fig.6 and in Table I.

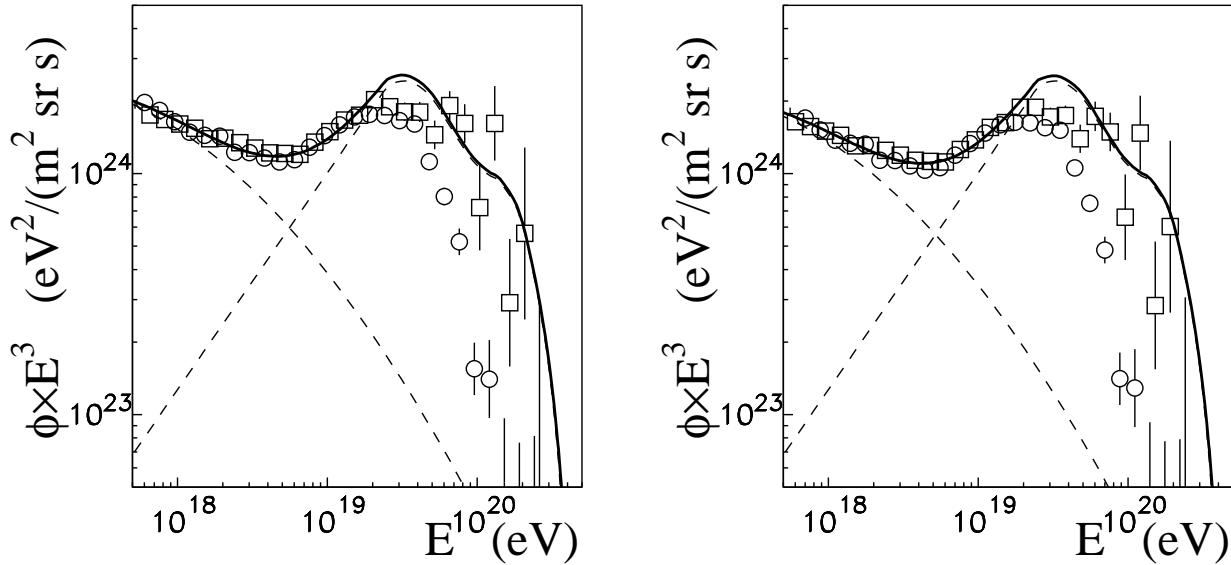


FIG. 5. Fits of our model parameters in the whole energy range to the spectra measured by PAO and TA. Left and right plots are as in Fig.4. The symbols are 'unfolded' with the universal spectrum shown as a black solid lines. The EG component is of the form of power-law with the high energy cut described in the text.

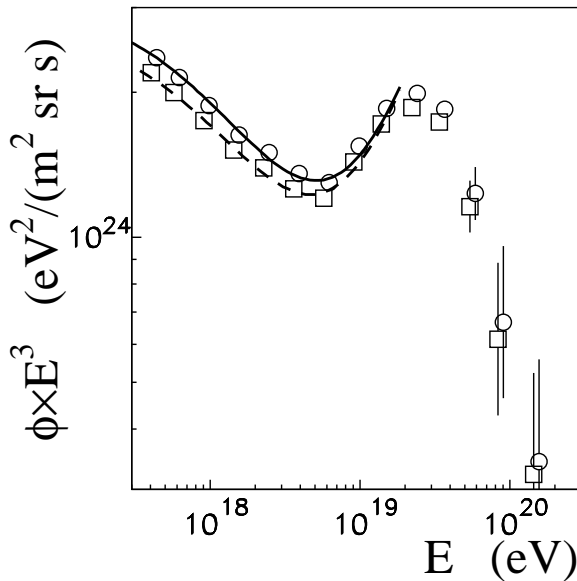


FIG. 6. The 'world average' UHECR spectrum. The circles and squares are combined PAO and TA results with the PAO and TA normalization used, respectively. The solid line is the ankle part of the universal UHECR spectrum with PAO normalization, the dashed line shows the TA normalization fit to the ankle.

IV. UHECR MASS COMPOSITION

With the 'world average' UHECR spectrum we tried to perform the mass composition estimation of "the end of the cosmic ray spectrum".

With the number of the model parameters increased by the fractions of each kind of nuclei (we limited ourselves

TABLE I. Universal UHECR spectrum for two energy normalizations.

Energy bin	PAO normalization	TA normalization
	$\log_{10}(\text{Flux} \times E^3)$	$\log_{10}(\text{Flux} \times E^3)$
17.4 - 17.6	24.296 ± 0.015	24.264 ± 0.015
17.6 - 17.8	24.254 ± 0.008	24.223 ± 0.013
17.8 - 18.0	24.196 ± 0.011	24.165 ± 0.011
18.0 - 18.2	24.135 ± 0.014	24.104 ± 0.008
18.2 - 18.4	24.098 ± 0.019	24.067 ± 0.013
18.4 - 18.6	24.055 ± 0.016	24.024 ± 0.008
18.6 - 18.8	24.036 ± 0.016	24.004 ± 0.008
18.8 - 19.0	24.112 ± 0.017	24.080 ± 0.012
19.0 - 19.2	24.191 ± 0.013	24.158 ± 0.007
19.2 - 19.4	24.222 ± 0.018	24.192 ± 0.012
19.4 - 19.6	24.189 ± 0.013	24.162 ± 0.009
19.6 - 19.8	24.014 ± 0.060	23.987 ± 0.054
19.8 - 20.0	23.747 ± 0.166	23.712 ± 0.158
> 20.0	23.458 ± 0.218	23.431 ± 0.210

to five groups of nuclei only) for both: G and EG components we are dealing with almost 20 parameters space for the minimization. It is obviously easy to reproduce the 14 points of the 'world average spectrum' even if some of the parameters are highly correlated. However, we have another two sets of observables of extensive air showers which are closely related to the mass composition: the $\langle X_{\text{max}} \rangle$ - average depth of the shower development maximum and $\text{rms}_{X_{\text{max}}}$ - the width of the X_{max} distribution. PAO and TA published respective data [8, 11] and again some inconsistencies between PAO and TA data sets are seen. They do not allow us to make the 'world average' by averaging points of both experiments. We are going to use the data as they are. The uncertainties concerning the Monte Carlo predictions [1, 2, 12], differences between models of hadronic interactions, and possible experimental systematics make the analysis harder and sometimes even problematic, see e.g., [14, 16]. But in spite of all this there is the tendency in the observations and the general trends should be reproduced by the model to be accepted.

A. Distribution of the Extragalactic UHECR sources

To perform the mass composition analysis we have to take into account as much as we can the possible effects of processes leading to loss of cosmic ray particles energy throughout their path from the sources to us. As it was said the form of 'the end of cosmic ray spectrum' depends on the optical depth obtained by the integration of the energy losses with the distances CR travel which is weighted by the CR source distribution $d(R)$

$$\tau = \int dR \left(\frac{1}{E} \frac{dE}{dR} \right) \Phi_{\text{source}}(E) d(R), \quad (5)$$

where $\frac{1}{E} \frac{dE}{dR}$ are shown in Fig.3.

The most obvious, as a first approximation to be used, is the uniform CR source distribution. It is used in the recent PAO analysis [13]. We will test this possibility as the first try.

Looking more deeply, there are some constraints, mostly from the anisotropy measurement [27] that the number of UHECR sources close (within few Mpc from us) should be small, possibly even zero [28]. So, our second guess is the uniform distribution but only for distances greater than 50 Mpc with no sources within. Such solution agrees well with the observed lack of anisotropy. The less drastic modification is the distribution of 'colliding galaxies' from [29] presented in Fig.7a. Quite different is the proposition of Medina-Tanco in his analysis of the AGASA data [30] (shown in Fig.7b) it is based on counting galaxies in the catalogue of CfA Redshift Survey from 1998.

Counting of galaxy clusters in the vicinity of our Galaxy gives another more realistic distribution of possible UHECR sources. We followed here the work of Dudarewicz and Wolfendale [31] which used maps from [32] and this distribution is shown in Fig.7c.

Modification on larger scales in our analysis are represented by 'the cold dark matter distribution' from Ref. [33] (Fig.7d). Going further away we test the cosmological evolution models with galaxy clusters [34] (Fig.7e) and the

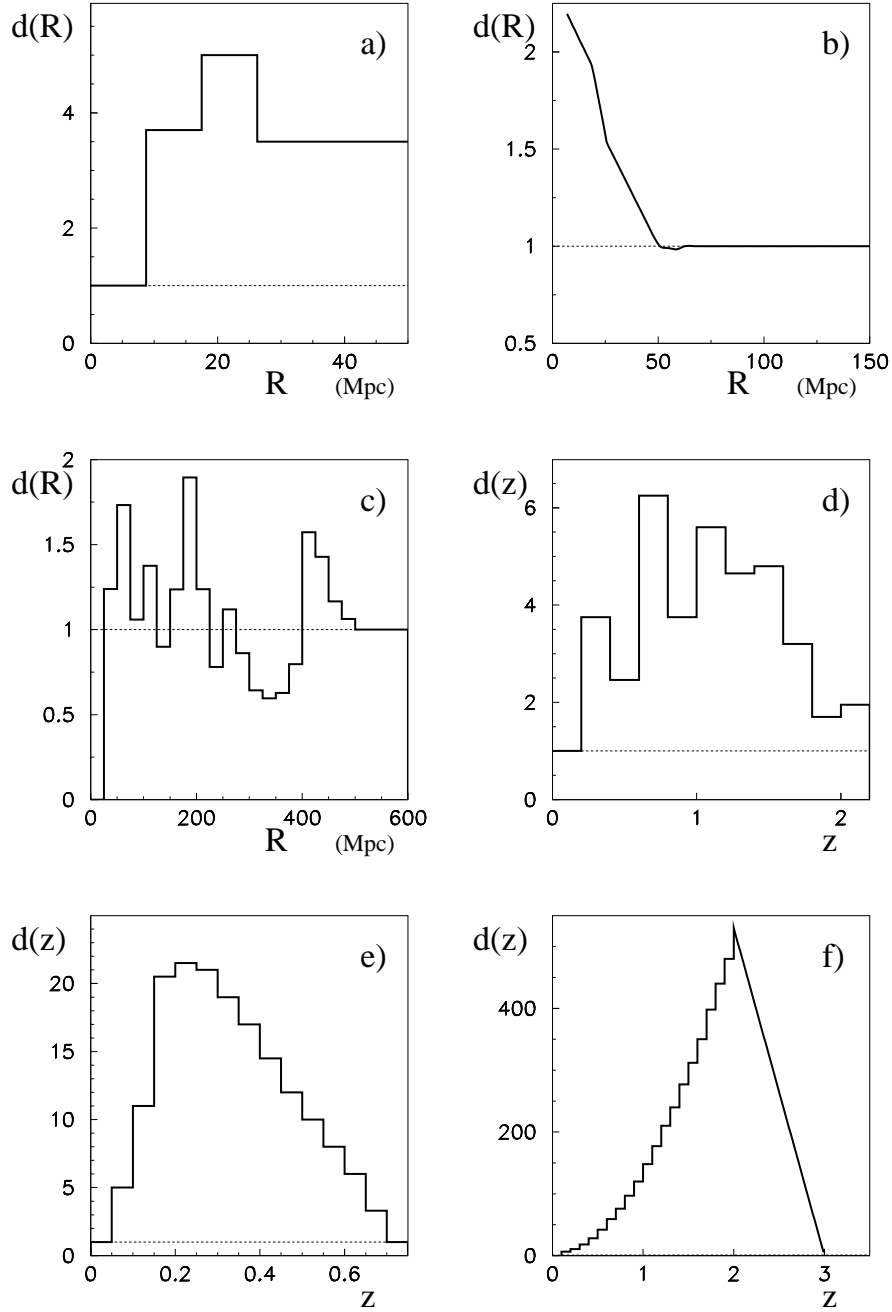


FIG. 7. Distribution of UHECR sources analyzed in the present work: a) - colliding galaxies [29] , b) - Medina-Tanco proposition [30], c) - DW [31], e) - CDM [33], f) - galaxy clusters [34] and g) - quasar distributions.

strong cosmological evolution models with $n= 5 - 6$ distribution motivated by distribution of quasars (Fig.7f). All the distributions (with some others) were examined by us in our earlier work [35].

The differences between models look huge but if we insert them to the Eq.(5) they become not so big. The large distances do not effect much the observed UHECR flux. Detailed results of cut-off factors are presented in Fig.8.

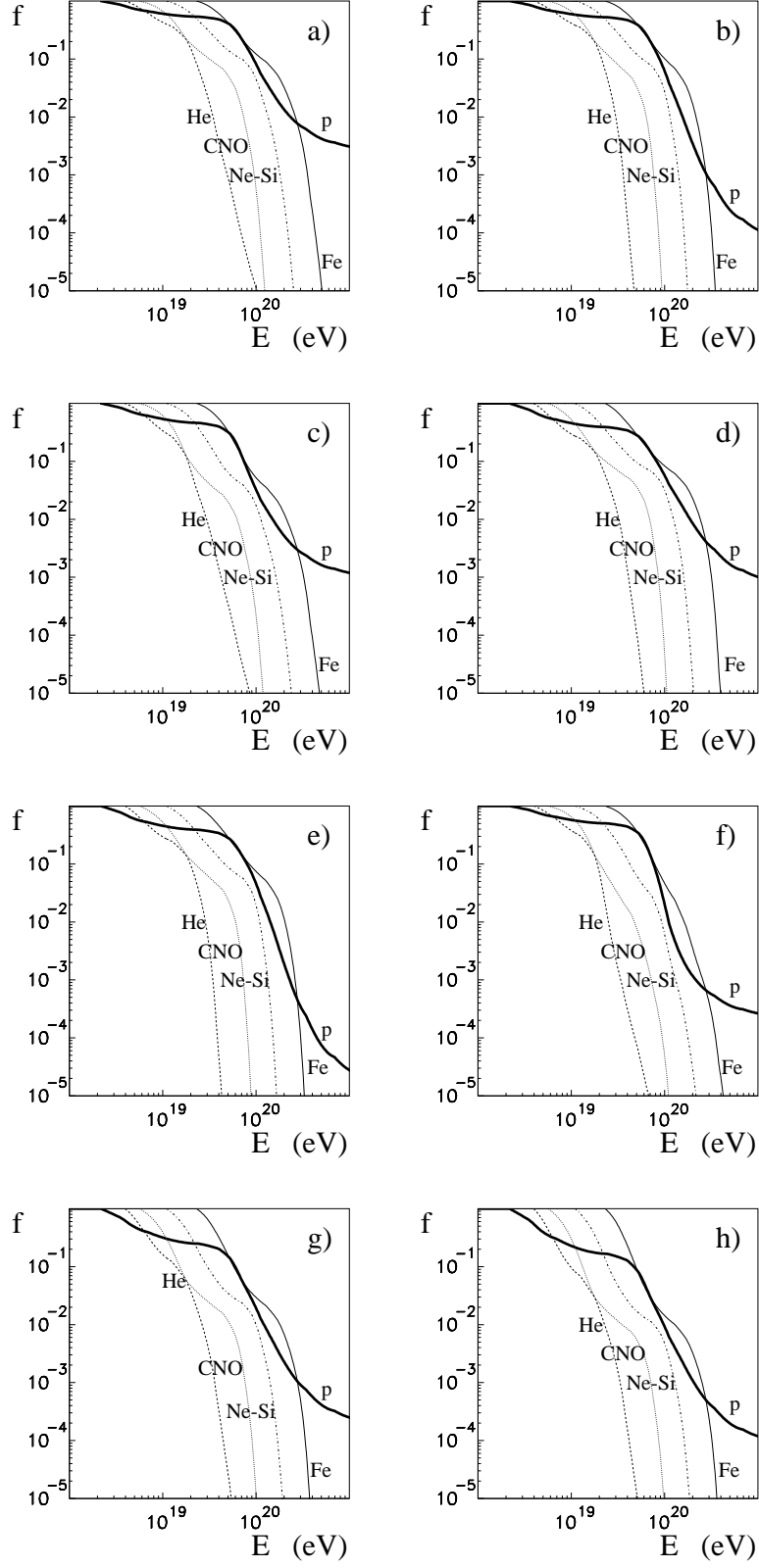


FIG. 8. Cut-off factors f of Eq.(2) calculated for different distributed CR sources: a) - uniform, b) - uniform but cut below 50 Mpc, c) - colliding galaxies, d) - Medina-Tanco, e) - DW, f) - CDM, g) - cluster of galaxies and h) quasar distributions.

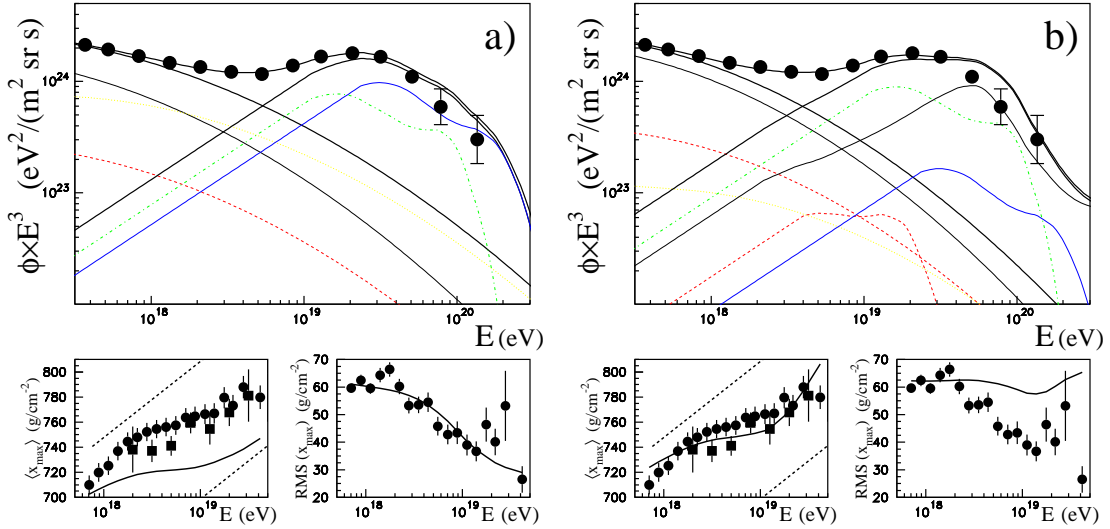


FIG. 9. Model predictions for the UHECR spectrum (top) and X_{\max} distribution data (bottom plots) with the $\langle X_{\max} \rangle$ data not included in the fit (left plots) and with the $\text{rms}_{X_{\max}}$ data not used for the fitting procedure (right plot).

B. Mass composition results

Cut-off factors presented in Fig.8 can be applied directly to the Eq.(2) and used for minimization of the χ^2 calculated for our ‘universal UHECR spectrum’ (Fig.6) and $\langle X_{\max} \rangle$ and $\text{rms}_{X_{\max}}$ data shown in Fig.2. The discrepancy between two experiments concerning measured X_{\max} distributions, but also the inconsistency of the simulation results concerning the $\langle X_{\max} \rangle$ and $\text{rms}_{X_{\max}}$ data, lead to the value of χ^2 out of any acceptable limits, however, this does not mean that the analysis has no real sense. The minimum χ^2 is still the measure of the ‘distance’ between theory (model) and experiment (data point). The real situation means only that the statistical interpretation of χ^2 is to be taken with care.

Fractions of all five groups on nuclei (p, He, CNO, Ne-Si, and Fe) for both Galactic and Extragalactic components were found together with the Galactic and Extragalactic model parameters:

- normalization (of the total Galactic flux) Φ_{0G}
- index γ_G
- position of the confinement cut-off for one of the component (Fe) $E_{G\text{cut,Fe}}$, with the respectively shifted (according to Z) values for other component fractions
- width of the confinement cut-off σ_G
- normalization (of the total Extragalactic flux) Φ_{0EG}
- index γ_{EG}

The strong binding of the model predictions by the ‘universal UHECR spectrum’ related to small uncertainties at each point is complemented with the requirement of keeping the slope of the spectrum around 10^{17} eV to be consistent with the data below the energy of 10^{18} eV can be seen in figures below. The additional simultaneous description of $\langle X_{\max} \rangle$ and $\text{rms}_{X_{\max}}$ data is, in principle, not possible, but we believe that there is possible to accept, in general, the proposed model leaving the more accurate solutions to the future works with improved simulations which have to be used for the interpretation of the shower development data.

The interesting exercise is to check the quality of the fits, if we diminish the weights for the $\langle X_{\max} \rangle$ data (neglecting them for the moment). The satisfactory agreement can be found both for spectrum and for the $\text{rms}_{X_{\max}}$ measurements. The $\langle X_{\max} \rangle$ data, of course, are then reproduces very bad (Fig.9a). On the other hand the reduction of the significance of $\text{rms}_{X_{\max}}$ allows us to find the good agreement for the spectrum and $\langle X_{\max} \rangle$ data, as seen in Fig.9b.

We would like to start our analysis from the examination of the effect of choosing different energy normalization: PAO and TA when the ‘universal UHECR spectrum’ is build. Fig.10 shows both cases: left is for the PAO normalization, right: for the TA one. For this comparison we used the uniform source distribution. Results, differences due

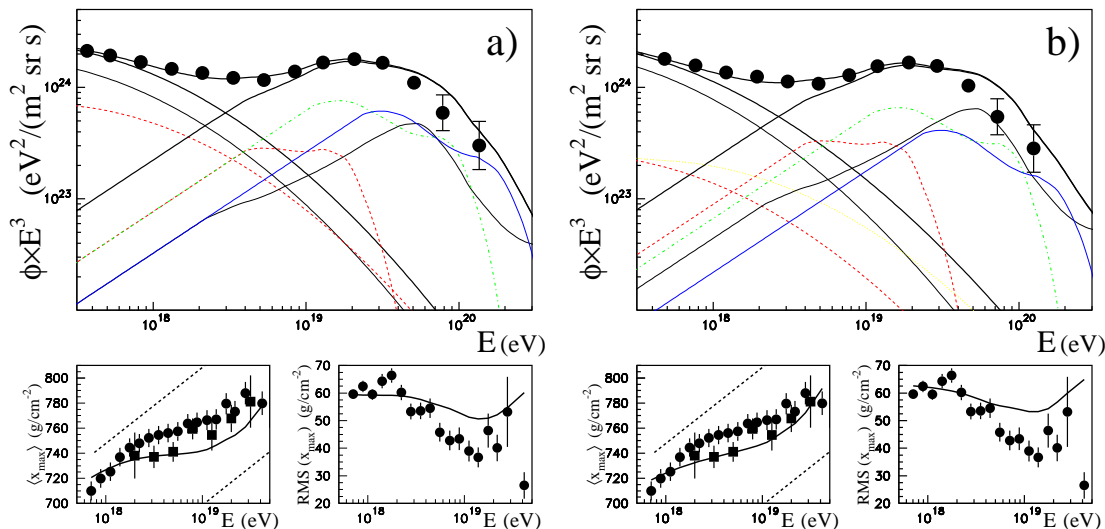


FIG. 10. Model predictions calculated uniformly distributed CR sources. For each case the energy spectrum is presented with the components shown separately as a tiny coloured lines (p- black solid, He- red dashed, CNO- yellow dotted Ne-Si- dash-dotted green, Fe- blue solid), average X_{\max} with two dashed lines representing simulation results for pure proton and iron predictions, and the r.m.s. of X_{\max} with solid line obtained with PAO simulations and dashed - with TA simulation predictions. Squares are the PAO measured point while circles are for TA data. Left plots are for PAO normalization while right plots for TA.

to the normalization, for other source distributions looks similar. The important conclusion concerning this point is a little surprising, but it looks like that the choice between PAO and TA normalization on the energy scale does not effect much the composition found. The differences are quite small and statistically not significant. For the PAO normalization the extragalactic component consists of about 0.5 of light fractions (p and He) and the same amount of heavies (Ne-Si and Fe) while for TA the ratio of light to heavy is 0.6 to 0.4.

Keeping this in mind we present in Fig.11 results of adjusting the source composition for all analyzed source distribution models obtained for PAO energy normalized ‘universal UHECR spectrum’.

In Fig.11 the separate nuclei components were plotted. We can see some differences there. Respective fractions of each group of nuclei in Galactic and Extragalactic UHECR flux are listed in the Table II. Fractions obtained with PAO normalization of the energy are given in the first row, while for TA energy normalization in the second row for each analyzed distribution.

Fractions shown in the Table II and individual element spectra shapes allows us to show the average mass of the UHECR as a function of the registered particle energy. Results are given in Fig. 12. The possible systematics related to the CR source distribution is space for the energies in the ankle region is of order of 20%.

V. DISCUSSION

In the paper [18] we have combined spectra obtained by five greatest experiment of these times Hi-Res, Fly’s Eye, Haverah Park, Yakutsk and AGASA using the idea of the universality of the feature called ‘the ankle’. We were able to describe the ‘universal spectrum’ obtained as the sum of Galactic and Extragalactic fluxes with significant fraction of heavy nuclei at the CR sources. We then put forward the question *At what particle energy do extragalactic cosmic rays start to predominate?* in Ref. [36] answering positively in the same paper. Further analysis confirmed this [33, 35] and with the first PAO results in Refs. [37, 38].

In the present paper which takes into account the recent data from PAO and TA experiments the ‘universal UHECR spectrum’ obtained using both measured spectra and additionally the X_{\max} results we confirmed the idea of exchanging the Galactic to Extragalactic CR flux at the ‘ankle’. The confirmation is made stronger by the composition data analysis which shows the significant fraction of heavy element above 10^{19} eV, above the ‘ankle’.

The ‘universal spectrum’ obtained in this work allows us to examine the distribution of Extragalactic sources of UHECR. Some models are more advantageous than others. The important contribution to the spectrum shape is the density of the EG sources in the vicinity (tens of Mpc) from Earth. The lack of galaxy clusters seen in [31, 32] shows the right directions to search for the UHECR sources, however the statistics of extremely high energy events is still

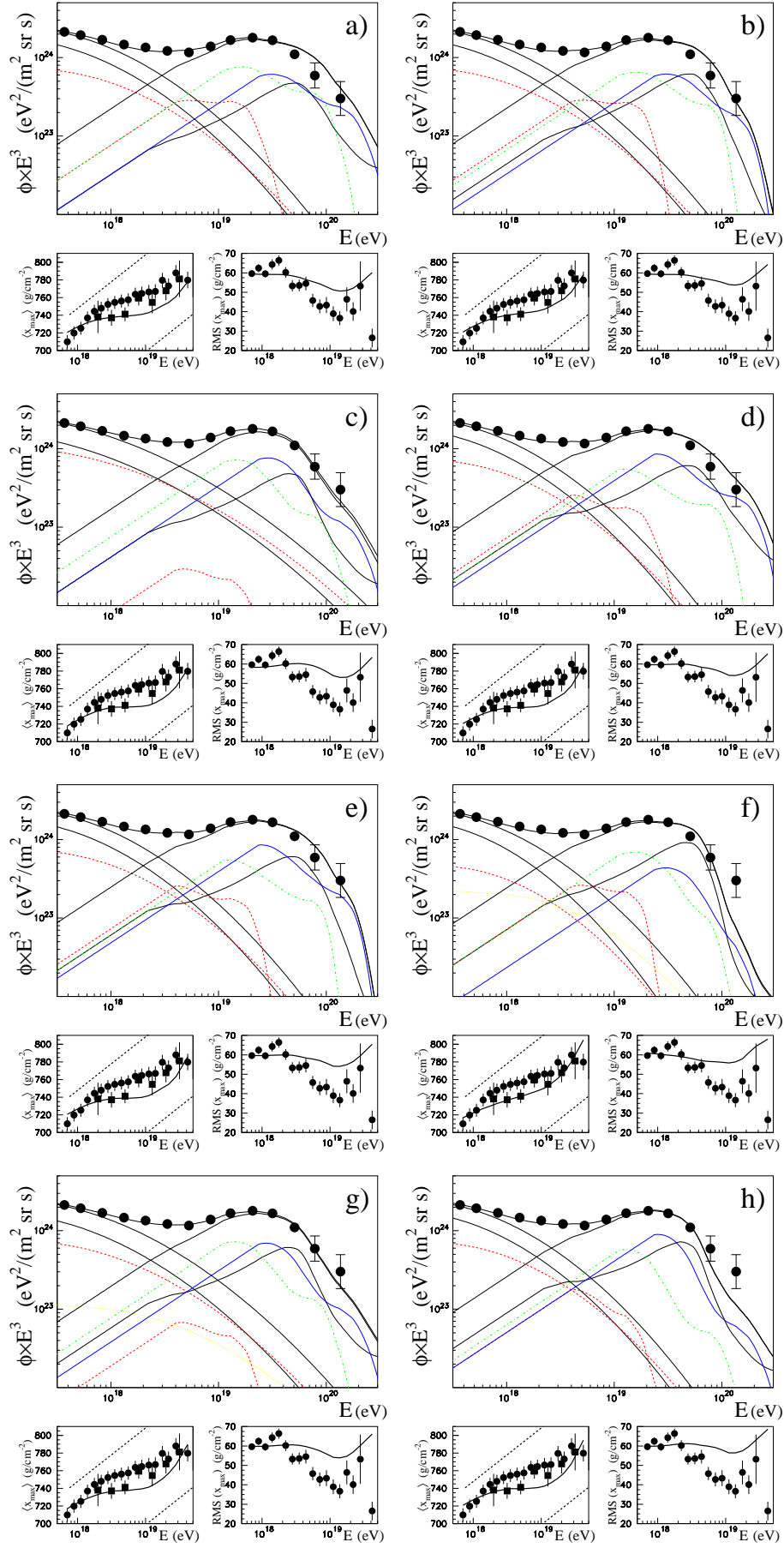


FIG. 11. Results calculated for different distributed CR sources: uniform (as shown in Fig.10 - left) - a), cut at 50 Mpc b), colliding galaxies c), Medina-Tanco proposition d), DW e), CMD f) cluster of galaxies g), and quasar h) distributions with PAO normalization.

TABLE II. Fractions of the Galactic and Extragalactic mass components for different source distributions and two normalizations of UHECR universal spectrum.

source distribution	Galactic					Extragalactic				
	p	He	CNO	Ne-Si	Fe	p	He	CNO	Ne-Si	Fe
uniform (PAO norm.)	0.70	0.30	0.00	0.00	0.00	0.15	0.35	0.00	0.35	0.15
	(TA norm.)	0.80	0.10	0.10	0.00	0.00	0.20	0.40	0.00	0.30
cut below 50 Mpc	0.70	0.30	0.00	0.00	0.00	0.20	0.35	0.00	0.30	0.15
	0.80	0.10	0.10	0.00	0.00	0.20	0.40	0.00	0.30	0.10
colliding galaxies [29]	0.60	0.40	0.00	0.00	0.00	0.25	0.05	0.00	0.45	0.25
	0.75	0.05	0.00	0.20	0.00	0.30	0.35	0.00	0.25	0.10
M-T [30]	0.70	0.30	0.00	0.00	0.00	0.25	0.30	0.00	0.25	0.20
DW [31]	0.70	0.30	0.00	0.00	0.00	0.25	0.35	0.00	0.25	0.15
	0.70	0.30	0.00	0.00	0.00	0.25	0.30	0.00	0.25	0.20
CDM [33]	0.70	0.30	0.00	0.00	0.00	0.25	0.25	0.00	0.35	0.15
	0.70	0.20	0.10	0.00	0.00	0.30	0.30	0.00	0.30	0.10
galaxy clusters [34]	0.70	0.30	0.00	0.00	0.00	0.15	0.20	0.00	0.45	0.20
	0.65	0.30	0.05	0.00	0.00	0.30	0.10	0.00	0.40	0.20
quasars	0.60	0.40	0.00	0.00	0.00	0.20	0.00	0.00	0.50	0.30
	0.70	0.30	0.00	0.00	0.00	0.35	0.20	0.00	0.25	0.20
	0.70	0.30	0.00	0.00	0.00	0.30	0.20	0.00	0.30	0.20

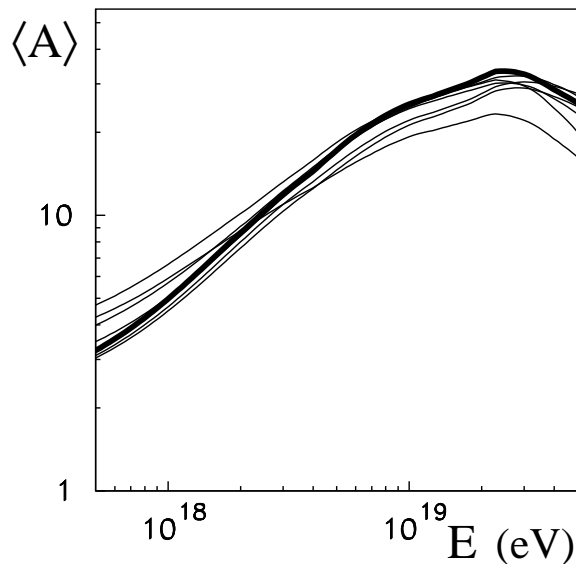


FIG. 12. Average UHECR particle mass as a function of particle energy. Each line represents different source distribution model analysed in this work. The differences are not big. The bold line is the result of the model Dudarewicz & Wolfendale [31].

too small to make the more definite statement.

We can compare our results with the main results of the PAO measurement of CR spectrum and shower development concerning the Extragalactic component shape and composition [13]. Using the uniform source distribution model (with the standard cosmological evolution) they conclude that the EG UHECR flux consists of heavy nuclei ($\sim 80\%$ of CNO and rest of Ne-Si group) with hard and very hard spectrum, $\gamma = 2.04 \pm 0.01$ ($\gamma = 0.96 \pm 0.1$ for the ‘main minimum’). We believe that their ‘second minimum’ (in the χ^2 search) is the real one. The value of the ‘main minimum’ is reported as ‘unexpected’ even by the Authors: Boncioli, di Matteo and Grillo from the Pierre Auger Collaboration [39]

in their paper title “*Surprises from extragalactic propagation of UHECRs*”). Such hard spectrum index is probably the effect of using the particular phenomenological model of EG component with the extra free parameter describing the rigidity dependent particle energy cut-off introduced alongside the known GZK and photodisintegration limits which work with no doubts at the very end of the cosmic ray spectrum. The very good agreement of the measured by PAO flux, and X_{\max} data with their model predictions is reported, and it is no surprise. The hard injection spectrum is obtained also in [40] where Unger, Farrar and Anchordoqui discussed their quite flexible model of the ‘ankle’.

The TA experimental team, following the HiRes Collaboration conclusions [12], reported rather opposite results concerning the UHECR mass composition. In Ref. [7] the TA Collaboration confirmed the HiRes and HiRes/MIA results indicate of $\sim 50\%$ of protons at 10^{17} eV, increasing to $\sim 90\%$ for energies above 10^{18} eV with the $+20\%–40\%$ uncertainty. This wide ‘error band’ accommodate almost all possible scenarios. The significant fraction of protons in the Galactic component is supported by the anisotropy results [41]. In Refs. [9, 17] TA spectra and X_{\max} data used as average values $\langle X_{\max} \rangle$ but also as the whole set of distributions in narrow energy bins favour clearly the pure proton cosmic ray flux at the whole energy range $10^{18}–10^{20}$ eV.

The analysis similar to the one presented above but only for the PAO results concerning the spectrum and X_{\max} data has been shown in Ref.[14] by Taylor, Ahlers and Hooper, in Ref. [15] by Hooper and Taylor and by Taylor in Refs.[21, 42]. One of the conclusions [42] is the significant fraction of medium light (CNO and Ne-Si) nuclei with the hard ($\gamma < 2$) injection spectrum. They studied also an interesting aspect, the effect of magnetic field strength (and structure) on the spectra (and anisotropy). In Ref. [43] Taylor, Ahlers and Aharonian the importance of nearby UHECR sources is analyzed. Their result of the absence of close ($R < 20–50$ Mpc) sources is to some extent confirmed by our calculations (the slightly better fit with the Dudarewicz & Wolfendale [31] model).

Globus, Allard and Parizot in [16] present the perfect agreement of the model they propose in the energy region of our interest with the PAO data on spectrum and X_{\max} . The model assumes the Galactic and Extragalactic UHECR components with mixed composition dominated by protons below 5×10^{18} eV then dropping to 10% at 3×10^{19} eV with introduction in the transition region of the dominated here CNO nuclei group. There are different spectra (slopes) for EG protons, and all other EG components: He, CNO and heavier nuclei up to Fe. With different source hardnesses and different cut-offs for each nuclei group the agreement in the ‘ankle’ region and above is not very surprising.

VI. CONCLUSIONS

We have examined the UHECR spectra measured by two big experiments The Pierre Auger Observatory and The Telescope Array Project. Both delivered numerous collections of events, the Extensive Air Showers initiated by ultra-high energy cosmic rays observed by arrays of ground detectors and by fluorescent light telescopes. The sophisticated technique used for their registration was complemented by complex procedures of the raw data correction and the corrected data evaluation to eventually form the reported UHECR particle energy spectra. The spectra measured in southern hemisphere by PAO and in northern by TA are displaced slightly both in the energy scale and on the intensity. This issue is known for years and is still standing open. We have tried to go through it and we obtained two solutions for the ‘world average’ UHECR spectrum with PAO and TA normalization, respectively. Some part of the discrepancy was reduced by adjusting possible, but a priori unknown difference in the individual shower energy reconstruction accuracy. It was estimated by both experimental group to be of order of 20%. After applying this procedure the difference in the energy normalization in both cases was found not to be as big as initially reported.

We then used both spectra for the further analysis of the mass composition. The study of UHECR energy spectrum alone, as it is mentioned already about 10 years ago in Ref. [44] can not give the definite, conclusive answer if the composition is heavy of light, or very light. Both proposition are acceptable. To find the answer one has to use the data on the shower longitudinal development. We have take them in the form of average depth of the shower maximum $\langle X_{\max} \rangle$ and its dispersion $\text{rms}_{X_{\max}}$.

We assumed that the UHECR flux is the sum of the the Galactic and Extragalactic components given by the simple (simplest?) form of power-laws at the sources with two indexes for Galactic of order of 3.1 and for Extragalactic of 2.1. Modified by the rigidity dependent confinement for the Galactic components and by the GZK or photodisintegration processes for the Extragalactic one.

Both components were assumed to be, in principle, mixtures of five group of nuclei from single nucleons, to iron nuclei. The four free parameters of each component (eight all together) were to be found comparing the model predictions with the PAO and TA data.

Our findings can be summarized as:

- the discrepancy of the energy scales between PAO and TA experiments does not effect substantially results of the mass composition of UHECR,
- the ‘universal UHECR spectrum’ can be reproduced for any reasonable source model distribution rather well,

- the light composition of the Galactic component of UHECR is mostly caused by the $\langle X_{\max} \rangle$ data of the PAO; it has to be remembered that this result is based strongly on the (PAO) shower simulations,
- the composition of extragalactic CR is heavier, it consists of about half of the Fe and Ne-Si group nuclei, but there is non negligible fraction of light elements, mostly protons and He, what is caused by the $\text{rms}_{X_{\max}}$ data,
- the medium CNO group of nuclei for both components, G and EG, is not needed at all to explain the data,
- the possible systematics of the source composition (the average mass) related to the CR source distribution for the energies in the ankle region is estimated to be of order of 20%,
- there is no possibility to answer definitely to the question of the distribution of the UHECR sources in space, but:
 - i) some recommendations can be given to the distribution without CR sources in the vicinity of the Earth, e.g., Dudarewicz & Wolfendale [31] or ‘colliding galaxies’,
 - ii) models assuming the strong cosmological evolution as ‘galaxy clusters’ and even more the ‘quasar’ model underestimates the flux above 10^{20} eV,
 - iii) the uniform CR sources distribution, and the proposition of Medina-Tanco [30] slightly overestimate UHECR flux at around 10^{20} eV,
- the common shape (the same slope) of the UHECR at the sources of the EG component leads to the definite difficulty with the explanation of the deep penetrating of UHECR in the atmosphere. It can suggest the needs of the revision of the ultra-high energy interaction model.

The last item is, maybe, the less conclusive, but in our opinion very important. The presented above short review of some ideas and quantitative analysis shows that further progress concerning the origin and nature of extremely high energy cosmic rays needs new insight to the very high energy interactions of nuclei which is not a simply, or not so simple, but still a superposition of many individual proton-proton multiparticle production processes. [45, 46].

-
- [1] P. Abreu *et al.* (Pierre Auger Collaboration), *Journal of Cosmology and Astroparticle Physics* **2013**, 026 (2013).
 - [2] A. Aab *et al.* (Pierre Auger Collaboration), *Phys. Rev. D* **90**, 122006 (2014).
 - [3] I. Valino *et al.* (Pierre Auger Collaboration), in *Proc. 34th ICRC*, The Hague, The Netherlands, PoS(ICRC2015)271 (2015).
 - [4] J. Abraham and P. Abreu, *Physics Letters B* **685**, 239 (2010).
 - [5] M. Settimo, *The European Physical Journal Plus* **127**, 87 (2012).
 - [6] D. Ivanov *et al.* (Telescope Array Collaboration), in *Proc. 34th ICRC*, The Hague, The Netherlands, PoS(ICRC2015)349 (2015).
 - [7] R.U. Abbasi *et al.* (Telescope Array Collaboration), *Astroparticle Physics* **80**, 131 (2016).
 - [8] T. Abu-Zayyad, *et al.* (Telescope Array Collaboration), *Astroparticle Physics* **64**, 49 (2015).
 - [9] P. Tinyakov, *Nuclear Instruments and Methods in Physics Research A* **742**, 29 (2014).
 - [10] T. Abu-Zayyad, *et al.* (Telescope Array Collaboration), *The Astrophysical Journal Letters* **768**, L1 (2013).
 - [11] A. Aab *et al.* (Pierre Auger Collaboration), *Phys. Rev. D* **90**, 122005 (2014).
 - [12] R.U. Abbasi *et al.* (The High Resolution Fly’s Eye Collaboration), *Phys. Rev. Lett.* **104**, 161101 (2010).
 - [13] A. Aab *et al.* (Pierre Auger Collaboration), *Journal of Cosmology and Astroparticle Physics* **2017**, 038 (2017).
 - [14] A. M. Taylor, M. Ahlers, and D. Hooper, *Phys. Rev. D* **92**, 063011 (2015).
 - [15] D. Hooper and A. M. Taylor, *Astroparticle Physics* **33**, 151 (2010).
 - [16] N. Globus, D. Allard, and E. Parizot, *Phys. Rev. D* **92**, 021302 (2015).
 - [17] Fukushima, Masaki *et al.* (Telescope Array Collaboration), in *Proc. 18th International Symposium on Very High Energy Cosmic Ray Interactions (ISVHECRI 2014)*, Geneva, Switzerland (2015) arXiv:1503.06961.
 - [18] J. Szabelski, T. Wibig, and A. Wolfendale, *Astroparticle Physics* **17**, 125 (2002).
 - [19] K. Greisen, *Phys. Rev. Lett.* **16**, 748 (1966).
 - [20] G. T. Zatsepin and V. A. Kuz’min, *Soviet Journal of Experimental and Theoretical Physics Letters* **4**, 78 (1966).
 - [21] A. M. Taylor, *The Propagation of Ultra High Energy Cosmic Rays*, Phd dissertation, University of Oxford (2006), a full PhD thesis entry: <https://ora.ox.ac.uk/objects/uuid:63572ebe-fb32-41b6-8b91-a7294db135a6>.
 - [22] D. Hooper, S. Sarkar, and A. M. Taylor, *Astroparticle Physics* **27**, 199 (2007).
 - [23] J. Linsley, *Phys. Rev. Lett.* **10**, 146 (1963).
 - [24] T. P. A. Collaboration, *Nuclear Instruments and Methods in Physics Research Section A: Accelerators, Spectrometers, Detectors and ...*
 - [25] M. Takeda *et al.*, *Astroparticle Physics* **19**, 447 (2003).
 - [26] H. Y. Dai, K. Kasahara, Y. Matsubara, M. Nagano, and M. Teshima, *Journal of Physics G: Nuclear Physics* **14**, 793 (1988).

- [27] P. Abreu *et al.* (Pierre Auger Collaboration), *Journal of Cosmology and Astroparticle Physics* **2012**, 040 (2012).
- [28] V. Berezhinsky, A. Gazizov, and S. Grigorieva, *Phys. Rev. D* **74**, 043005 (2006).
- [29] S. S. Al-Dargazelli, A. W. Wolfendale, A. Smialkowski, and J. Wdowczyk, *Journal of Physics G: Nuclear and Particle Physics* **22**, 1825 (1996).
- [30] G. A. Medina-Tanco, *The Astrophysical Journal Letters* **510**, L91 (1999).
- [31] A. Dudarewicz and A. W. Wolfendale, *Monthly Notices of the Royal Astronomical Society* **268**, 609 (1994).
- [32] R. B. Tully, R. Scaramella, G. Vettolani, and G. Zamorani, *Astrophys. J.* **388**, 9 (1992).
- [33] T. Wibig and A. W. Wolfendale, in *Proc. 30th ICRC*, Merida, Mexico, 269 (2007).
- [34] N. A. Bahcall, *Ann. Rev. Astron. Astrophys.* **26**, 631 (1988).
- [35] T. Wibig and A. W. Wolfendale, *Journal of Physics G: Nuclear and Particle Physics* **34**, 1891 (2007).
- [36] T. Wibig and A. W. Wolfendale, *Journal of Physics G: Nuclear and Particle Physics* **31**, 255 (2005).
- [37] T. Wibig and A. W. Wolfendale, in *Proc. 21st ECRS*, Kosice, Slovakia, 269 (2008) arXiv:0712.3403 [astro-ph].
- [38] T. Wibig and A. W. Wolfendale, *Astrophysics and Space Sciences Transactions* **7**, 275 (2011).
- [39] D. Boncioli, A. di Matteo, and A. Grillo, *Nuclear and Particle Physics Proceedings* **279**, 139 (2016).
- [40] M. Unger, G. R. Farrar, and L. A. Anchordoqui, *Phys. Rev. D* **92**, 123001 (2015).
- [41] P. G. Tinyakov, F. R. Urban, D. Ivanov, G. B. Thomson, and A. H. Tirone, *Monthly Notices of the Royal Astronomical Society* **460**, 3479 (2016), arXiv:1511.01333 [astro-ph.HE].
- [42] A. M. Taylor, *Astroparticle Physics* **54**, 48 (2014).
- [43] A. M. Taylor, M. Ahlers, and F. A. Aharonian, *Phys. Rev. D* **84**, 105007 (2011).
- [44] D. Allard, N. G. Busca, G. Decerprit, A. V. Olinto, and E. Parizot, *Journal of Cosmology and Astroparticle Physics* **2008**, 033 (2008).
- [45] A. Aab *et al.* (Pierre Auger Collaboration), *Phys. Rev. Lett.* **117**, 192001 (2016).
- [46] A. Aab *et al.* (Pierre Auger Collaboration), *Phys. Rev. D* **91**, 032003 (2015).